

VLBI TRACKING OF THE HUYGENS PROBE IN THE ATMOSPHERE OF TITAN

S. V. Pogrebenko^(J,1), L. I. Gurvits^(J,2), R. M. Campbell^(J,3), I. M. Avruch^(J,4),
J.-P. Lebreton^(E,5), C. G. M. van't Klooster^(E,6)

^(J)Joint Institute for VLBI in Europe, 7991 PD, Dwingeloo, The Netherlands

^(E)ESA-ESTEC, 2200 AG, Noordwijk, The Netherlands

E-mails: ⁽¹⁾pogrebenko@jive.nl ⁽²⁾lgurvits@jive.nl ⁽³⁾campbell@jive.nl ⁽⁴⁾avruch@jive.nl
⁽⁵⁾jean-pierre.lebreton@rssd.esa.int ⁽⁶⁾Kees.van.t.Klooster@esa.int

ABSTRACT

We present results of an assessment study of VLBI (Very Long Baseline Interferometry) observations of the Huygens probe during the probe's descent through the atmosphere to the surface of Titan [1]. The aim of the study was to assess the feasibility of a direct receipt, detection and VLBI processing of the probe's S-band radio signal. The direct receipt of the probe signal by Earth-based tracking stations was not foreseen in the original mission scenario but has proven to be possible owing to recent developments in radio astronomy, and particularly in VLBI. We analyze the power budget of the "Huygens-Earth" radio link, the potential accuracy of the VLBI determination of the probe's coordinates in the atmosphere of Titan, and some scientific applications of these measurements. We also discuss prospects for VLBI tracking of future deep space missions using the next generation Earth-based radio telescopes, in particular the Square Kilometer Array (SKA).

1. INTRODUCTION

VLBI tracking of the Huygens probe in the atmosphere of Titan is based on the possibility to determine the angular position of a source of radio emission with an accuracy of the order of

$$\Delta j \cong \frac{1}{SNR} \frac{I}{B} \quad (1)$$

where I is the signal wavelength, B is the radio interferometer baseline, and SNR is the signal-to-noise ratio of the detected interferometric response. At the S-band frequency of 2 GHz and global baselines of the order of the Earth's diameter, the achievable accuracy is at the milli-arcsecond (mas) level. With $SNR \sim 20$ -30 or more this corresponds to a sub-km accuracy of the probe position at the distance to Titan at the time of Huygens-Titan encounter, ~ 8 astronomical units (AU).

Recent developments in the techniques of VLBI permit us to achieve this level of accuracy.

To derive the probe's position from the detected VLBI responses, the so-called phase-referencing technique [2] must be applied. This technique is based on the determination of the telescope phase offsets and propagation phase distortions by observing known bright references sources, deriving the phase corrections from these, and applying them to the data of a weaker target source. The achievable accuracy of phase calibration depends on the signal-to-noise ratio of the interferometer response to the calibrator source and its angular distance from the target. The most efficient use of phase referencing would be realised if both the target and reference source(s) were within the primary beams of all the participating radio telescopes. Nevertheless, it has been proven [3, 4] that this switching technique works at angular separations between reference and target sources of up to several degrees, although it is less accurate as compared to 'in-beam' technique, depends on atmospheric conditions, and requires 'nodding' of telescopes between target and reference sources, which decreases the observing efficiency.

For the purpose of our experiment we are focusing on detection of the probe's narrow band signal carrier wave, because it represents the signal component with the maximum spectral power density and can provide the best possible signal-to-noise ratio. On the other hand, observations of calibrators require as wide a bandwidth as possible to achieve the desired accuracy. Digital disk-based VLBI recorders such as Mk5 [5] will allow us to record the signal from both the probe and the calibrator onto the same medium, to ensure the coherency of phases between these two signals.

Observations of the probe's descent will be performed using VLBI telescopes capable of receiving the probe's signal at 2.040 GHz (with original receivers or specially tuned ones), although the telescopes equipped with standard S-band VLBI receivers (typically

covering the frequency band above 2.2 GHz) will be used as well, in order to improve the phase calibration accuracy.

To process the data, we will need both wide bandwidth processing facilities for the calibrators' signals and ultra narrow band processing tools for the probe's signal. The EVN Mk4 VLBI correlator at JIVE [6] can process the broad band data from as many as 16 VLBI stations simultaneously, and can be enhanced with ultra-high spectral resolution hardware/software tools for narrow-band processing.

2. PROBE'S SIGNAL DETECTABILITY AND ESTIMATE OF THE TRACKING SNR

The effective isotropic power of the probe's Channel A transmitter is 10.2 – 11.0 W, and the transmitting antenna gain is 3.44 dBi (worst case scenario) in a 120 degrees cone [7]. The modulation scheme PM/BPSK/PCM-NRZM with 1.34 radians modulation index produces an output of ~7 W in a data band, and leaves ~3.5 W in a carrier wave. This yields a carrier wave signal power density (flux) at Earth (distance 8.2 AU) of $P_s=4.8 \text{ W/m}^2$.

The typical spectrum of a BPSK signal is shown in Fig.1. The data band with a 16 Kbps capacity is separated from the carrier by 130 KHz, which makes the carrier wave very well isolated from the data band and suitable for a high resolution radio spectroscopic analysis.

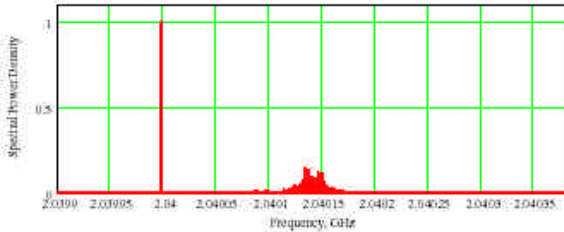


Fig.1. Typical spectrum of the BPSK modulated signal.

The intrinsic width of the carrier line is determined by the stability of the on-board Ultra Stable Oscillator – USO. The Allan variances for the Huygens USO [8] are presented in Table 1.

Table 1. The Huygens USO Allan variances

Integration time [s]	$\Delta f_0 / f_0$
0.1	$6 \cdot 10^{-11}$
1	$1 \cdot 10^{-11}$
10	$5 \cdot 10^{-12}$
100	$1 \cdot 10^{-12}$

The good short-term stability of USO (Allan variances floor is below 10^{-12} at 100 s) allows us to search for the monochromatic spectral component in the received signal with up to a 100-10 mHz resolution or 10-100 s effective coherent integration time, provided the probe's Doppler shift and long-term frequency drifts of the USO (caused by aging and thermal, acceleration and pressure variations [8]) are modeled and compensated. For initial detection of the signal a shorter integration time will be required, of the order of 1 s, with an effective spectral resolution of the order of 1 Hz.

High resolution spectral analysis combined with proper phase correction of the received signal can yield a detection SNR at a single station with antenna diameter D , aperture efficiency A_{eff} , system temperature T_{sys} , coherent integration time t_{int} and frequency resolution dF , ($dF = 1 / t_{int}$):

$$SNR = A_{eff} \frac{P D^2}{4} \frac{P_s}{k T_{sys}} \frac{1}{dF} \quad (2)$$

where P_s is the carrier wave flux at Earth and k is Boltzmann's constant. Expected SNR values for different integration times for a set of typical telescopes which can *in principle* observe the Huygens probe are listed in Table 2.

Table 2. Expected detection SNRs for typical stations at different integration times.

Station	D (m)	A_{eff}	T_{sys} (K)	SNR 1s	SNR 10s	SNR 100s
GBT	100	0.71	23	7.70	77.0	770.0
Parkes	64	0.55	35	1.50	15.0	150.0
Usuda	64	0.55	40	1.45	14.5	145.0
VLBA_OV	25	0.55	30	0.29	2.85	28.5
VLBA_SC	25	0.48	40	0.19	1.95	19.5
Kashima	34	0.65	75	0.25	2.50	25.0
Mopra	22	0.60	37	0.19	1.96	19.6
Kashima_11	11	0.80	72	0.03	0.33	3.30

A signal-to-noise ratio SNR_{XY} on a baseline between telescopes X and Y in the case of a point source and perfect phase calibration is

$$SNR_{XY} = \sqrt{SNR_X SNR_Y} \quad (3)$$

where SNR_X and SNR_Y are those for stations X and Y . The results for cross-correlation SNRs for 8 typical stations (the same as listed in Table 2) and 50 s

coherent integration time ($df=20$ mHz) are listed in Table 3.

Table 3. Baseline SNR's for 50 s coherent integration on various baselines.

Stations	1	2	3	4	5	6	7
1 GBT							
2 Parkes	170						
3 Usuda	167	74					
4 VLBA_OV	74	33	32				
5 VLBA_SC	61	27	26	12			
6 Kashima	69	31	30	13	11		
7 Mopra	61	27	27	12	10	11	
8 Kashima_11	25	11	11	5	4	5	4

Estimated baseline SNR's are acceptable, even for small 11m antennas, when correlated against 100 or 64 meter class antenna. This leaves us with the key issue of achieving an adequate phase calibration accuracy.

3. GLOBAL VLBI STATIONS SUITABLE FOR OBSERVATIONS OF THE PROBE

At 09h ET on the 14th of January 2005, the Huygens probe is scheduled to start its transmission. About 70 minutes later the signal will reach the Earth. Fig.2 illustrates how the Earth will be visible from Titan during the probe's descent in the atmosphere.

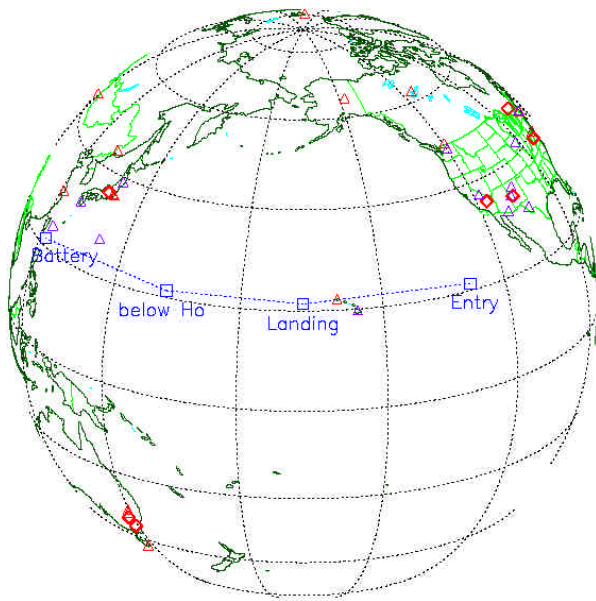


Fig.2. Earth as seen from Titan at the moment of Huygens probe's landing. Sub-Titan points of the "observed" moments of entry, Cassini going below the probe's horizon and full battery budget are also shown.

During the probe's descent, Titan will be visible by Australian, Chinese, Japanese and US radio telescopes. European IVS station Ny Alesund will also see Titan. It is essential that at the beginning of the observations the probe will be visible by two large telescopes, GBT and Usuda. After an hour and a half Titan will go below the horizon for the GBT and other Eastern USA telescopes but will appear above the horizon for Australian telescopes such as Parkes, Mopra, Hobart and EVN telescopes at Shanghai and Urumqui (China). At the end of the expected probe's battery life the signal could be received by European telescopes such as Effelsberg, Ny Alesund and Onsala. Potentially, the longest possible global baselines can be achieved during the whole duration of the mission.

About 30 VLBI stations around the world could participate in the Huygens observations, provided they are equipped with 2.04 GHz receivers and disk based data recorders. Of course, the actual observing network is subject to special considerations.

4. CELESTIAL BACKGROUND AROUND THE HUYGENS-TITAN ENCOUNTER POINT

In order to conduct a phase-referencing VLBI observation of the Huygens probe, it is essential to know the exact (at the milliarcsecond level) positions and flux densities of calibrator sources.

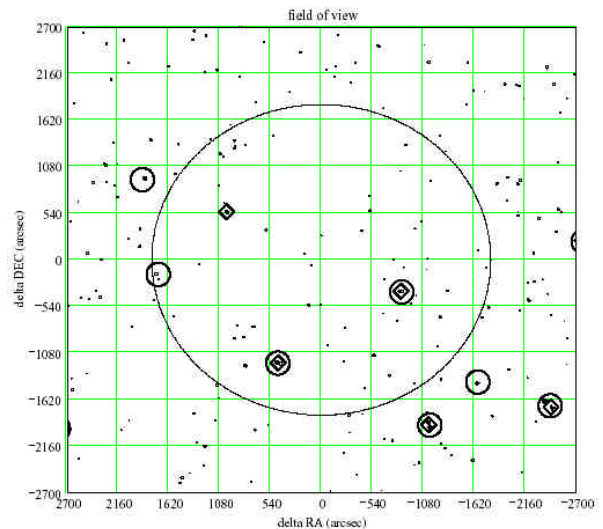


Fig.3. Known radio sources around the point of Huygens-Titan encounter. The FIRST survey detection – small dots, the Texas survey data – diamonds and GBT data – circles.

In preparation for the observations we have examined published catalogs for radio sources in the target field; at low frequencies (400 MHz and below): the Texas survey [9], the B2 catalog [10], the 4C [11] and Culgoora [12] surveys; at L-band: the VLA FIRST [13] and NVSS [14] catalogs; at C-band: MGI [15], BWE

[16], 87GB [17], and the GB6 [18] catalogs; and at X-band the JVAS [19] and Patnaik [20] surveys. Fig. 3 shows the known radio sources in an area of 1.5 by 1.5 degrees. A circle with radius of 30 arcminutes indicates the area of particular interest, which can be considered the typical isoplanatic patch at S-band.

There are three JVAS sources at distances 1.7 – 3 degrees from the encounter center. They are bright enough (150, 250 and 1200 mJy) to be used as primary calibrators, although for more accurate phase calibration closer sources are preferable [4]. Multiple calibrators closer to the target center allow us to calibrate the phase gradients and further improve the accuracy.

There are 68 FIRST sources with flux densities in the range of 1 - 180 mJy in the 1 degree diameter area. Four of the sources in the field were also detected with the Texas and GBT surveys, although with a rather higher detection limit and lower spatial resolution.

We have initiated pre-VLBI, high sensitivity, multi-frequency observations of the field at frequencies 0.8, 1.8, 2.3, 4.8 and 8.4 GHz in order to identify flat or gigahertz-peaked spectrum sources as possible VLBI calibrators. Fig.4 illustrates an example of such multi-frequency and morphological analysis – VLA maps of the radio source J0743+2103 at 1.4 GHz (left) and 8.4 GHz (right) with a compact flat spectrum core. This source is at a distance of 22 arcmin from the target and is a potential calibrator.

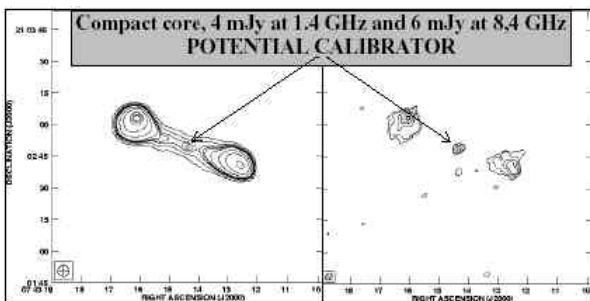


Fig.4. VLA radio maps of J0743+2103 at 1.4 GHz (the FIRST survey) and 8.4 GHz (project AC406).

5. THE ARCHITECTURE OF THE HUYGENS PROBE SIGNAL PROCESSING

The architecture of the Huygens probe VLBI data processing is based on an extension of the EVN Mk4/Mk5 correlator at JIVE.

It is essential for the project that signals from both the probe and the calibrators are recorded onto the same standard VLBI recording medium. Mk5 disk based VLBI recorder/playback units [5], which are currently in use at some of the EVN and IVS VLBI stations, are

capable of recording radio signals at a data rate of up to 1 Gbps for several hours. The K5 system used in Japan has similar characteristics. Tools for data exchange between MK5 and K5 units have been developed at CRL (Japan) [21].

The EVN Mk4/Mk5 VLBI data processor at JIVE [6] is currently equipped with 16 Mk4 tape based playback units and 4 fully operational MK5 disk based units. Two more MK5 units are in the process of system integration. The correlator itself is capable of processing 256 MHz bandwidth of data from up to 16 VLBI stations simultaneously; mixed tape/disk playback and processing is also possible. Fig. 4 shows the block diagram of the EVN correlator data/control flow and its extension for the Huygens probe signal processing.

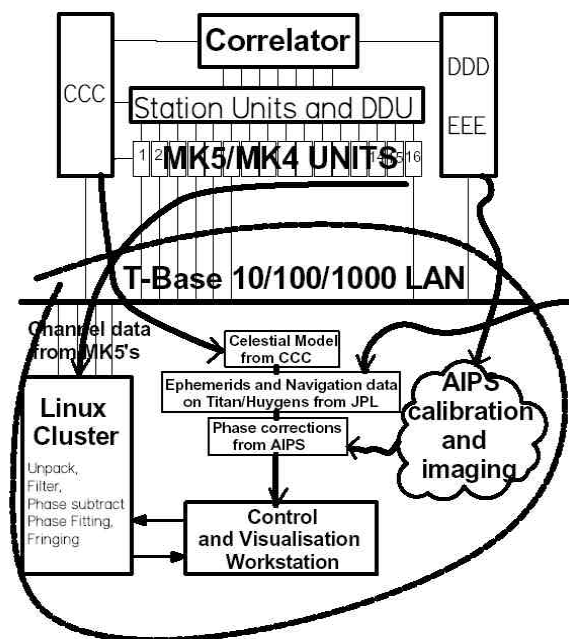


Fig.4. Block diagram of the EVN correlator at JIVE (at top) and its extension for the Huygens signal processing (encircled area at the bottom).

It is a challenging task to process both the narrow band data from the Huygens probe and the broad band data from phase calibration radio sources with adequate accuracy and mutual phase coherence.

At a full bandwidth of 256 MHz and 16 stations, the EVN correlator is able to achieve spectral resolution of the order of 100 KHz, while for the probe detection we need something 5-6 orders of magnitude better, although in a much narrower total bandwidth.

Possible solutions is to download a 16 MHz-wide channel of data from the MK5 units into a powerful

general purpose computer, i.e. a Linux cluster, filter the bandwidth down to a level acceptable from the point of view of initial Doppler shift uncertainties, and then process it in a phase referencing spectroscopic mode. The required spectral resolution of 1 Hz, for primary detection with the biggest radio telescopes, and 10 - 20 mHz resolution for final tracking on all the stations is then a matter of software.

Within this architectural solution, the processing algorithm is as follows:

1. Broad-band correlation of the calibrators' signals using the EVN correlator with a standard setup.
2. Fringe fitting, calibration and mapping of the calibrators' data using the Astronomical Image Processing System (AIPS). Obtaining a phase correction model for each radio telescope.
3. Download of the 16 MHz channel data from Mk5s to the Linux cluster.
4. Application of a nominal geocentric Titan motion Doppler shift model based on the JPL ephemeris. Filter down the bandwidth of data to about 10 KHz which corresponds to +/- 600 m/s velocity uncertainty. Apply the nominal telescope motion models, narrowing down the bandwidth to 4 KHz or +/- 300 m/s, which will cover the most extreme motion model residuals.
5. Apply the multitude of possible probe trajectories, based on different atmospheric and parachute performance models with a residual uncertainty of about 5-10 m/s. That will allow us to see the signal on dynamic spectra from the largest (100 to 64 m diameter) telescopes.
6. Phase-lock the motion model to the detection, applying the individual telescope phase corrections derived from calibrators' images, narrowing down the bandwidth to about 10 Hz and frequency resolution to about 50 mHz, and confirming the visibility of the signal at 25 - 30 m class antennas. At a frequency resolution $\delta F > 30 - 40$ mHz, there will be no significant phase difference between data from different telescopes, so only the radial velocity model, common for all the telescopes, needs be applied.
7. At the next step, it will be necessary to fit a model of 3-dimensional motion, consider the differential phases between telescopes caused by tangential motion of the probe, and include more telescopes into the analysis. Phase fitting can run iteratively in a loop to improve the frequency resolution and SNR until the final accuracy is achieved.

5.1 Ultra-high spectral resolution correlation test

We have performed a test in order to check the data consistency when transferring raw VLBI data from the Mk5 unit, and control parameters (telescope motion models) from the Correlator Control Computer (CCC) into a general purpose computer running a specially designed ultra-high spectral resolution software correlator. The spectral resolution of 8 Hz (1 million spectral bins) achieved over the 8 MHz wide band is close to that required for the probe's signal detection. Fig. 5 illustrates the test correlation results for the radio source DA193 (flux density 5 Jy at 5 GHz) on the EVN baseline Effelsberg–Medicina, observed on 02.06.2003 and processed on 27.09.2003. Comparison of the achieved SNR with the SNR obtained during the standard processing with the EVN correlator shows perfect consistency.

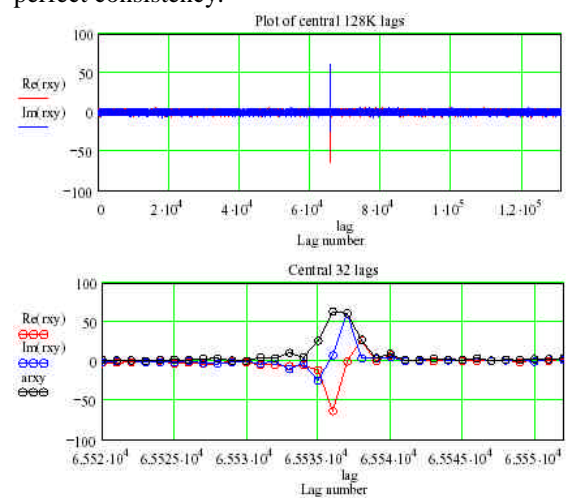


Fig.5. VLBI response (cross-correlation function) of the ultra-high spectral resolution software correlator.

6. NUMERICAL SIMULATION OF THE PROBE VLBI TRACKING

In order to verify the expected accuracy and technical details of the above described data processing algorithm, we performed a numerical simulation of global VLBI observations of the Huygens probe. The model network included 24 telescopes: NRAO and IVS stations (USA and Canada) and CRL, GCI, NAOJ and ISAS stations (Japan). Although not all of these stations are currently equipped with 2.04 GHz receivers, we included them in the model to investigate a potentially achievable performance. Since the simulation covered about 1 hour of probe observations, ATNF stations (Australia) were not included in the model.

We used nominal parameters for each station, such as coordinates, antenna diameters, aperture efficiencies and system temperatures as published on the respective

station websites. The probe's transmitter power and antenna gain were taken from [7].

The received signal voltage for each telescope was calculated according to the signal flux at Earth, P_s , the telescope's diameter D and aperture efficiency A_{eff} . Noise voltages were modeled as Gaussian noise with a power corresponding to the T_{sys} of the given telescope.

To model the intrinsic phase pattern of the probe's USO we used its Allan variances and environment-dependent characteristics, such as ageing, temperature, pressure and magnetic field susceptibilities [8]. A random phase behavior pattern was created using a spectral shaping algorithm based on [22].

For a geometrical phase behavior estimate, we modeled the probe's motion in a geocentric coordinate system and calculated the phases of arriving signals for each telescope (including USO phase drift and a random walk model). Phases corresponding to a motion of a nominal pointing centre were calculated separately and subtracted from that of the "true" probe's motion. To better illustrate these considerations one can say that the pointing centre motion model may represent the motion of an arbitrarily selected point on Titan's surface. Fig.6 illustrates the vector model used for phase calculations.

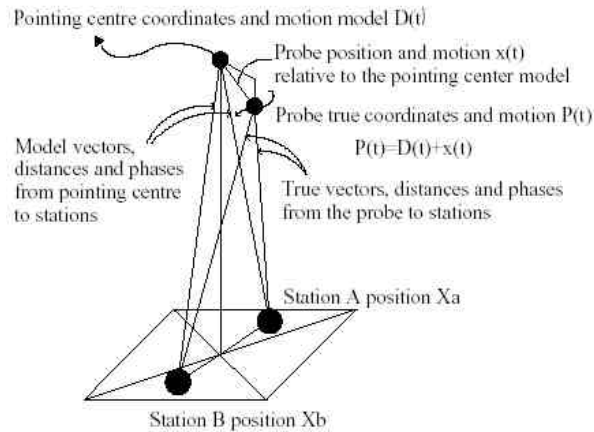


Fig.6. Geometry of the motion model.

A 3-dimensional relative motion model included two components: trend and random walk, with an amplitude of random walk velocity of about the same value as the trend velocity for all three coordinates; a characteristic velocity scale for radial motion (Z) was 3 m/s and for tangential motion (XY) 100 m/s. Within the simulation time of 3200 s, XY motion covered an area 300 km square.

Such a motion can fit into 40 Hz of Doppler uncertainty bandwidth, although for real data processing with a powerful computer this bandwidth

can be much wider, covering velocity uncertainty of tens of meters per second.

We started processing of the modeled signals with a spectral analysis of this 40 Hz band. Fig. 7 presents dynamic spectra for GBT, Usuda and VLBA_OV stations with 1.25 Hz resolution, 0.8 s integration time per spectrum and 3200 s total time span. We used 50% overlapping of data samples for each spectrum and 4 - fold FFT super resolution for better sampling for subsequent fitting of the frequency/phase model to the spectral data. At this resolution, signals were seen only by the two largest telescopes. A 20-th order Chebishev polynomial fit to the frequency/phase curve worked well for both GBT and Usuda.

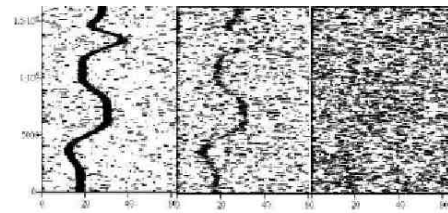


Fig.7. 1.25 Hz resolution dynamic spectra for GBT, Usuda and VLBA_OV stations.

Next, the phase curve derived from the 1.25 Hz resolution spectra was subtracted from the data, the bandwidth was narrowed and signals were processed with a 0.312 Hz resolution (3.2 s coherent integration time). Fig.8 illustrates the results. At this resolution the probe's signal is clearly visible with a 25m/30K-class antenna (VLBA_OV).

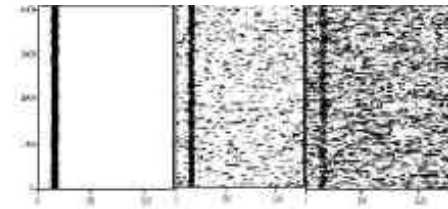


Fig.8. Dynamic spectra with 312 mHz resolution after fitting the phase model from the 1.25 Hz spectra. Stations (from left to right): GBT, Usuda, VLBA_OV.

Iteratively, with subsequent fitting of phase residuals, a frequency resolution of 40 mHz (25 s coherent integration time) was achieved. At this resolution the signals are clearly visible with ~20 m and 40-50 K class antennas (IVS stations Kookee Park and Westford) and can even be traced in the data from a 11m/70K class antenna (CRL station Kashima_11). The resulting spectra for these 3 antennas are presented in Fig.9.

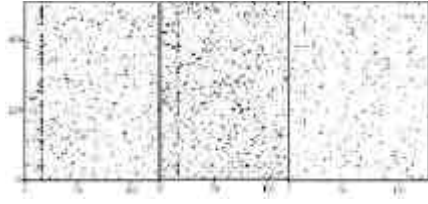


Fig.9. 40 mHz resolution dynamic spectra for 22, 18 and 11 m class antennas.

We stopped the single-station spectral analysis at this resolution, because tangential motion with a velocity of ~100 m/s induces a differential phase rate on global baselines of the order of 5 mHz. This differential phase rate can be included into the full 3-D phase fit or derived directly from the spectral analysis of cross-correlated baseline data. However, we proceeded to direct cross-correlation of the 40 mHz data and subsequent mapping of the probe's motion.

Mapping is a straightforward process, given calibrated visibilities (cross-correlation coefficients) at a sufficient number of baselines. Fig.10 illustrates the final result for 20-station mapping: the XY position of participating telescopes on the geocentric plane, the input and recovered probe's trajectory, residual errors of the tangential coordinates recovery, and reconstructed radial velocity compared to that input. Results correspond to 25 s coherent integration and uncoherent smoothing with a 100 s Gaussian kernel.

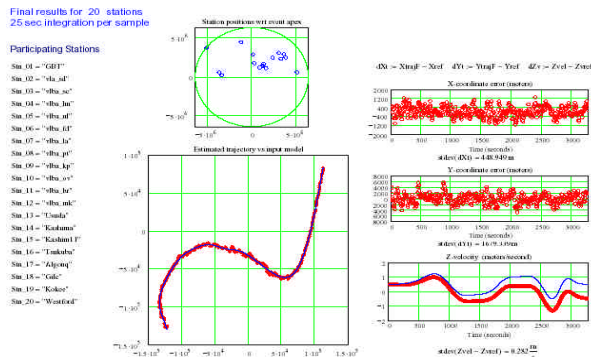


Fig.10. Results of simulated tracking of the probe's motion.

With these stations, the longest East-West baseline was between VLBA St.Croix and CRL Kashima, and the longest North-South baseline between IVS Gilmore Creek and VLBA Mauna Kea. Residual errors for the probe's positioning are < 300 m in East-West direction and < 1000 m in North-South. Radial velocity reconstruction error is < 0.3 m/s and is mainly due to long term USO frequency drift and temperature instability.

We note that additional inclusion in the VLBI array of radio telescopes in Australia is highly desirable, and

would significantly improve the sensitivity and angular resolution comparing to figures shown above, especially 1-1.5 hours after the interface time, when Titan will be below horizon for the telescopes on the East Coast of the US (GBT and others).

7. VLBI CONTRIBUTION TO THE HUYGENS MISSION SCIENTIFIC RETURN AND THE PROSPECTS FOR FUTURE EXPERIMENTS

As shown above, VLBI tracking of the Huygens probe during its descent through the atmosphere of Titan, would yield independent direct detection of the probe's signal on Earth and 3D determination of the probe's position in the ICRF frame every 10-30 seconds. These data will directly impact the interpretation of all other measurements on-board the probe. They also provide a useful synergy to the Doppler measurements of the Huygens motion both from the Cassini spacecraft and ground based stations.

As it is clear from the study described in this paper, VLBI tracking of Watt-level transponders at the distances of the order of 10 AU is a challenging but realistic task for present day VLBI technology. The critical parameter determining feasibility of such observations is sensitivity of the VLBI array. In the coming decades this parameter is likely to improve dramatically, due to the implementation of the next generation radio telescope - the Square Kilometre Array (SKA, [23]). VLBI tracking of Deep Space missions anywhere in the Solar System would be a suitable task for the SKA, after its full implementation around 2020.

8. CONCLUSIONS

The explanatory study described here allows us to conclude the following:

1. Highly accurate VLBI measurements of the probe trajectory in the atmosphere of Titan are possible. The expected accuracy of the absolute (linked to the ICRF) position on XY plane is < 1 km and radial velocity < 1 m/s, on a time scale of 1 minute.
2. A true 3D model of the Huygens motion can be reconstructed if VLBI and DWE data are combined together.
3. VLBI tracking will increase the synergy of the scientific return of the mission.
4. The potential to maintain radio contact with the probe after the link with the orbiter has been broken (when the Cassini orbiter goes below the probe's horizon) has been demonstrated.

5. The tracking potential of current and future VLBI instruments for planetary and deep space mission support has been demonstrated.

To implement these results into a “live” VLBI Huygens experiment the following is required:

1. To organise a global VLBI network of radio telescopes for Huygens probe observations, optimal in terms of performance/complexity/cost.
2. To perform a series of pre-interface deep medium-resolution and VLBI observations of the target field; create a reference astrometric-accurate radio map for phase-referenced VLBI observations of the event.
3. To develop adequate hardware and software solutions for processing of Mk5 recorded probe signals and mixed media (disk/tape) observations.
4. To perform VLBI observations of the probe’s descent, process the data and reconstruct the probe’s motion model with the highest achievable accuracy.

We believe that this project will pave the way for future VLBI navigation observations of planetary and deep space missions, using the current VLBI network and new radio astronomical instruments under development.

9. ACKNOWLEDGEMENTS

This study was conducted at the Joint Institute for VLBI in Europe under the ESA contract No. 17002/02/NL.

This research has made use of the SIMBAD database, operated at CDS, Strasbourg, France and the NASA/IPAC Extragalactic Database (NED) which is operated by the Jet Propulsion Laboratory, California Institute of Technology, under contract with the National Aeronautics and Space Administration.

We express our thanks to J. Buitter, M. Leeuwinga, A. Szomoru, S. Parsley, H. van Langevelde and M. Garrett (JIVE) for support, MK5 hardware/software handling and useful, constructive, and inspiring discussions. We also are grateful to M. Perez Ayucar (ESA/ESTEC) for his explanatory contribution and useful discussions regarding technical details of the Huygens probe.

10. REFERENCES

1. Gurvits L. I. et al. VLBI observations of the Huygens probe. Assessment study report. *JIVE research note #0004*, 10.07.2003.

2. Alef W. Introduction to phase-referencing, *Very Long Baseline Interferometry, Techniques and Applications*, NATO ASI Series, Kluwer, 261, 1989.
3. Beasley & Conway, ASP Conf. Series #82.237, 1995
4. Garrett M.A. et al. EVN Observations of the Hubble Deep Field. *Astron. & Astrophys.*, 366, L5-8, 2001.
5. Whitney A. et al. Mark 5 Project Home Page. <http://web.haystack.mit.edu/mark5/Mark5.htm>
6. Schilizzi R. T. et al. The EVN-MarkIV VLBI data Processor. *Experimental Astronomy*, 12, 49-67, 2001.
7. Cassini/Huygens, Integrated Data Report, *ESA-JPL-HUY-25999*, 2002.
8. Bird M. K. et al, The Huygens Doppler Wind Experiment, *ESA series SP-1177*, 139-162, 1997.
9. Douglas J. N. et al. The Texas survey of radio sources covering $-35.5^\circ < \delta < 71.5^\circ$ at 365MHz. *Astron. J.* 111, 1945, 1996.
10. Colla G. et al. A catalogue of 3235 radio sources at 408 MHz. *A&A. Suppl. Ser.* 1, 281, 1970.
11. Pilkington J. D. H. and Scott P. F. A survey of radio sources between declinations 20 and 40. *Mem. R. Astron. Soc.*, 69, 183-224, 1965.
12. Slee O.B. Radio Sources Observed with the Culgoora Circular Array (CCA) at 80 and 160 MHz. *Australian J. Phys.*, 48, 143-186, 1995.
13. Becker R.H. et al. The FIRST Survey Catalog, *Astrophys. J.* 475, 479, 1997.
14. Condon J.J. et al. The NRAO VLA Sky Survey. *Astron. J.* 115, 1693, 1998.
15. Bennett C.L. et al. The MIT-Green Bank (MG) 5GHz survey. *Astrophys. J. Suppl. Ser.* 61, 1 1986.
16. Becker R. H. et al. A new catalog of 53522 4.85GHz sources. *Astrophys. J., Suppl. Ser.* 75, 1-229, 1991.
17. Gregory P.C. and Condon J.J. The 87GB Catalog of Radio Sources covering 0 to $+75^\circ$ at 4.85 GHz. *Astrophys. J. Suppl. Ser.* 75, 1011-1291, 1991.
18. Gregory P.C. et al. The GB6 catalog of radio sources. *Astrophys. J. Suppl. Ser.* 103, 427, 1996.
19. Wilkinson P. N. et al. Interferometer phase calibrations sources. *Mon. Not. R. Astron. Soc.*, 300, 790-816, 1998.
20. Patnaik A.R. et al. Interferometer Phase Calibration Sources. *Mon. Not. R. Astron. Soc.* 254, 655, 1992.
21. Koyama Y. International eVLBI experiments. http://www2.crl.go.jp/ka/radioastro/tdc/news_21/pdf/koyama.pdf 2002.
22. Rogers A. E. E. and Moran J. M. Coherence limits for Very-Long-Baseline Interferometry. *IEEE Transactions on Instrumentation and Measurement*. Vol. IM-30, No 4, 283, 1981.
23. Taylor R. A. The Square Kilometre Array: A Science Overview. In *Perspectives on Radio Astronomy: Science with Large Antenna Arrays*, ed. Haarlem M. P., Astron publications, 1-10, 1999.